Bioelectromagnetics 16:197–206 (1995)

Measurement and Analysis of Static Magnetic Fields That Block Action Potentials in Cultured Neurons

A.V. Cavopol, A.W. Wamil, R.R. Holcomb, and M.J. McLean

Departments of Neurology, Vanderbilt University Medical Center (A.V.C., A.W.W., R.R.H., M.J.M.), Department of Veterans Affairs Medical Center (M.J.M.), and Holcomb Technologies, Inc. (R.R.H.), Nashville, Tennessee

To characterize the properties of static magnetic fields on firing of action potentials (AP) by sensory neurons in cell culture, we developed a mathematical formalism based on the expression for the magnetic field of a single circular current loop. The calculated fields fit closely the field measurements taken with a Hall effect gaussmeter. The biological effect induced by different arrays of permanent magnets depended principally on the spatial variation of the fields, quantified by the value of the gradient of the field magnitude. Magnetic arrays of different sizes (macroarray: four center-charged neodymium magnets of ~14 mm diameter; microarray: four micromagnets of the same material but of ~0.4 mm diameter) allowed comparison of fields with similar gradients but different intensities at the cell position. These two arrays had a common gradient value of ~1 mT/mm and blocked >70% of AP. Alternatively, cells placed in a field strength of ~0.2 mT and a gradient of ~0.02 mT/mm produced by the macroarray resulted in no significant reduction of firing; a microarray field of the same strength but with a higher gradient of ~1.5 mT/mm caused ~80% AP blockade. The experimental threshold gradient and the calculated threshold field intensity for blockade of action potentials by these arrays were estimated to be ~0.02 mT/mm and ~0.02 mT, respectively. In conclusion, these findings suggest that spatial variation of the magnetic field is the principal cause of AP blockade in dorsal root ganglia in vitro.

Key words: static magnetic fields, spatial field variation, computer model, gradient, action potential blockade, cultured sensory neurons

INTRODUCTION

Electrically stimulated action potentials of adult mouse sensory neurons in cell culture were blocked to a large extent when the neuron was positioned in a static magnetic field of ~11 mT intensity produced by an array of four permanent magnets of alternating polarity [McLean et al., 1991, 1995]. In the original experiments, the magnitude of this biological effect depended on positioning of the neuron under study in the field (changes in vertical distance of cell from the array), on array parameters (e.g., action potential blockade decreased with increasing distance between magnets in the array), and on the number and polarity of the magnets in the array. To facilitate description of the field properties that determined the biological effect, we have developed a mathematical formalism that closely simulates the experimental field measurements. Computer-assisted modeling facilitates a comprehensive algebraic characterization of the field properties. Here we compare field characteristics of different arrays to identify possible correlations between field structure and the corresponding AP blockade.

MATERIALS AND METHODS

The methods regarding cell culture, action potential recording and data analysis have been published previously[McLean et al., 1991, 1995].

Received for review April 15, 1994; revision received October 10, 1994.

Address reprint requests to Michael J. McLean, MD, PhD, Department of Neurology, Vanderbilt University Medical Center, 2100 Pierce Avenue, 351 MCS, Nashville, TN 37212.

Magnetic Field Measurements

The magnetic field produced by arrays of cylindrical neodymium magnets (radius a = 7 mm and height h = 5 mm, referred to as *macroarray*) was measured with a gaussmeter (see Appendix) model 4048 (F.W. Bell, Newton, MA). The probe was attached to an x,y,z, mechanical micromanipulator, and the fields were scanned from the surface of the magnet outward along the z axis at 1 mm increments and sideways in the other two dimensions at a constant height, z = 6 mm, for all three field components B_x, B_y, and B_z (Fig. 1). The three scanning directions intersected at a site corresponding to the cell position in the field. With reference to the center of the array, designated (x,y,z) = (0,0,0), the cell position throughout the experiments was in the range(x,y,z) = (0 ± 1 mm, 4.5 ± 1 mm, 6 ± 1 mm). Positioning of the magnets and the experimental apparatus have been described in detail elsewhere [McLean et al., 1991, 1994].

For some experiments, magnets of radii a = 0.2 mm and height h = 1 mm were used to construct microarrays with an overall diameter of ~0.8 mm. Some dimensions relevant to the microarray experiments are given for future reference: The neuronal diameter was $\Phi_{CELL} \approx 40$–60 μm and the physical microarray area diameter was $\Phi_{ARRAY} \approx 800$ μm. The neuron under study was positioned at a height h = 1.5 ± 0.2 mm above the array. Positioning in the horizontal plane was difficult due to the small size of the array. Positioning variability contributed to a wide range of effects on action potential firing (see Discussion and Appendix). The background magnetic field and its variation over the cell culture dish were below 1 gauss.

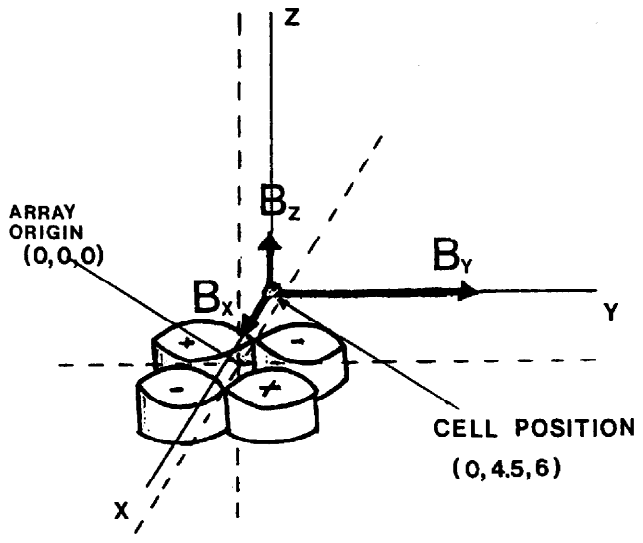

Fig. 1. Coordinate system of the experimental setup. Field components were scanned along x,y,z axes intersecting at a location corresponding to the experimental position of the cell; with the center of the array as the origin, cells were positioned within the range (x,y,z) = (0 ± 1 mm, 4.5 ± 1 mm, 6 ± 1 mm).

Experimental Error

A detailed error analysis is presented in the Appendix. Measurement errors were caused mainly by vernier reading error, by imperfect superposition of the coordinate systems of the magnet and the micromanipulator arm holding the probe, and by gaussmeter reading error, which was considered small compared to the other two. Another experimental limitation comes from the field averaging performed by the gaussmeter due to the size of the measurement window of the Hall probe.

Computer Model

A computer model of array magnetic fields supplements our measurements, allows three-dimensional graphic display of the fields and makes quantitative analysis of field characteristics possible. To preserve relative algebraic simplicity, we assume that the field of a cylindrical magnet can be described by the magnetic field of a current loop (magnetic dipole) [Landau and Lifschitz, 1969]. The field generated by a four-magnet array is obtained by superposition of the four individual dipole fields. The resultant total field is characterized by three parameters: a = radius of the magnet, 2c = distance between adjacent magnet centers, and m = a scaling factor.

RESULTS

Theoretical Fit

Plots of experimental data and simulations based on these data were within the experimental measurement error for most of the domain. For a parameter setting that corresponds to the physical magnet dimensions (a = c = 7 mm), the field amplitude has been set to match the peak value of the experimentally measured component B_{xz}. This sets the value for the scaling parameter m (m = 43) and completely specifies the theoretical field, which is then compared to the remaining components of the experimental field. As an example, the fit between the measured and computed values of the x component of the field is shown in Figure 2. The computer model closely reproduces all the experimental field measurements (additional data available upon request), especially in the data collection range (0 ± 1 mm, 4.5 ± 1 *mm*, 6 ± 1 *mm*) where field variations are linear. Computed values for the y and z components fit the measured data equally well. This validates use of the computer model as an analytic tool to describe the global characteristics of the field.

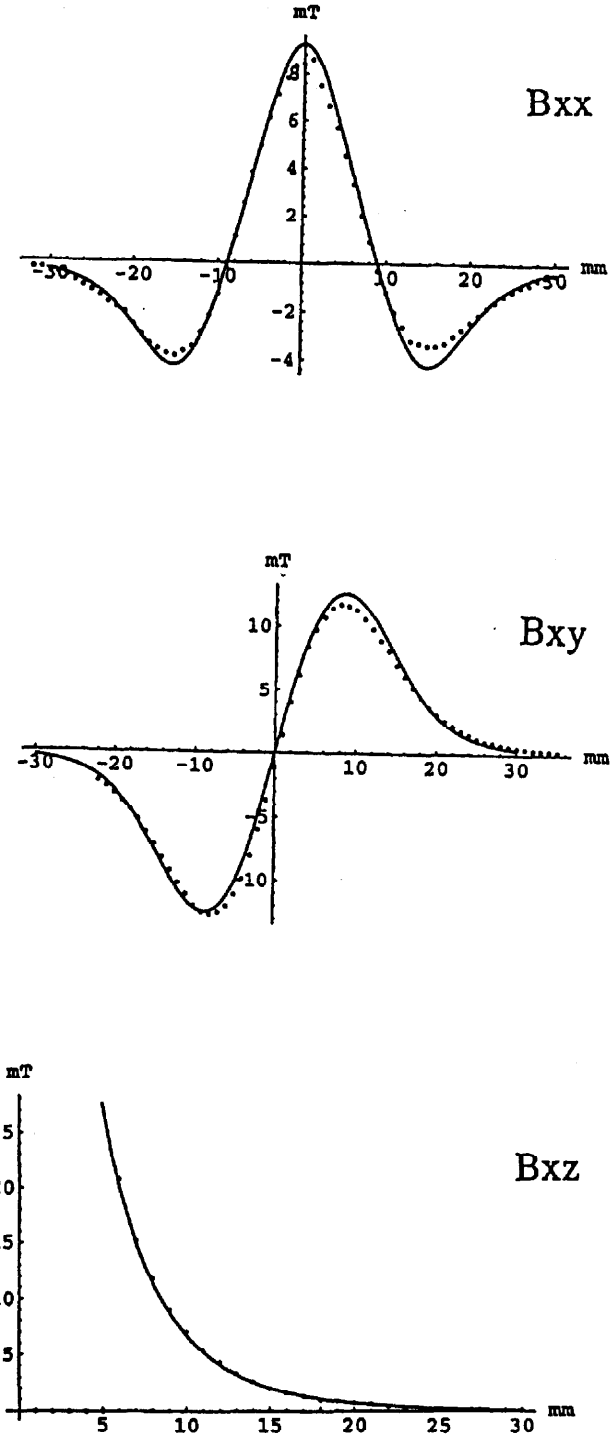

Fig. 2. Comparison between the experimental data points (dotted line) and curves calculated on the basis of a current loop model (solid line) for the x component of the magnetic field of the MAG-4A array. In the notation B_{ij}, i labels the field component and j the scanning direction. Domains and ranges were chosen to demonstrate the fit.

Effect of Spatial Field Variation

The effect of static magnetic fields produced by arrays of four magnets of alternating polarities (MAG-4A), arrays of four magnets of the same polarity (MAG-4+) and arrays of two magnets of alternating polarity (MAG-2A) on AP firing is displayed in Figure 3 (top row). All arrays were constructed of magnets of the same material, shape, and dimensions. The maximum field strengths for the different kinds of arrays were within 10% of one another. The number of stimuli that failed to elicit action potentials depended on the number and polarity of magnets in the array. Computer simulations in the middle and bottom rows in Figure 3 show the spatial variations of the field magnitudes of the three arrays. The slope of the inner cone, determined from two of the three field variations that define the gradient,[1] can be taken as a visual correlate of the gradient. The gradient of the field magnitude, a global measure of spatial field variation, was used to compare the different arrays quantitatively. The number of AP failures and duration of the blockade were highest for the MAG-4A, which had the steepest gradient at cell position. These findings indicate that, under similar peak intensity conditions, the spatial distribution of the field strength determines the extent of the blockade.

To reduce the number of physical parameters that influence the biological effect, we designed MAG-4A experiments to test the correlation between the strength of the spatial variation of the field and the extent of the neural effect. The principal field determinant of AP blockade was separated by controlling the values of field intensity and the magnitude of the gradient for the MAG-4A arrays. Due to the limited number of sizes and strengths of available permanent magnets, field strength and variation were controlled by adjusting the distance between magnets in the macroarray and use of a MAG-4A microarray.

Arrays with similar field gradients but significantly different field intensities.

At a height z = 1.5 mm corresponding to the cell position in the field, the microarray (see Materials and Methods), field magnitude ranges between background and ~0. 1 mT, and the gradient ranges from a minimum of 0.1 mT/mm to a maximum of ~2 mT/mm (Table 1). The small volume of the microarray magnets results

[1]The term *gradient* refers to the gradient of the field magnitude, B_{MAG}, and the numerical values given refer to the magnitude of the gradient and are calculated according to the formula:

$$|\mathrm{Grad}(B_{MAG})| = \sqrt{\left(\frac{\partial B\ MAG}{\partial x}\right)^2 + \left(\frac{\partial B\ MAG}{\partial y}\right)^2 + \left(\frac{\partial B\ MAG}{\partial z}\right)^2}.$$

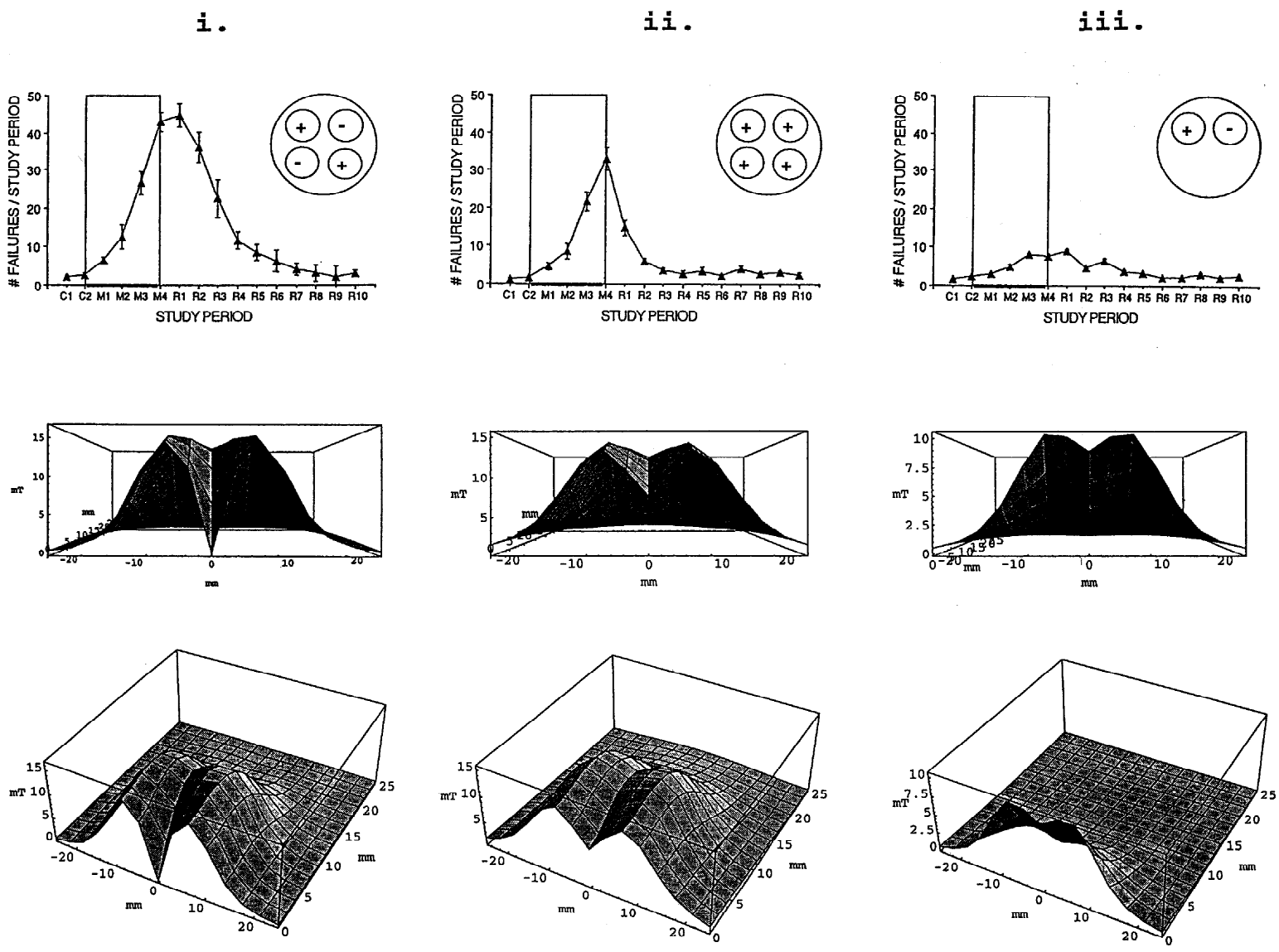

Fig. 3. Correlation between the number of AP failures and spatial variation of fields produced by three arrays of permanent magnets: 1) four magnets of alternating polarity (i.), 2) four magnets of the same polarity (ii.), and 3) two magnets of alternating polarity (iii.). Top row: Plots of data showing numbers of AP failures for C-like neurons measured at cell location for the different arrays. A stimulus protocol consisting of two control (C1, C2), four magnetic exposure (M1–M4), and up to 10 recovery (R1–R10) periods (50 stimuli at 1 Hz) was used. Boxes outline the period of exposure to the magnetic field. Cell location is (x,y,z) ~ (0,5,6 mm), with the origin at the center of the four-magnet array. Same origin for the two-magnet array, taken as half of the four-magnet array. Data from McLean et al. [1994], reexpressed graphically. Bottom rows: Corresponding plots of field magnitude in the xy plane at z = 6 mm. The gradient of the field magnitude is proportional to the slope of the sectional cut in row 2, which describes the field variation in the xy plane. The variation of the field magnitude along the z direction (not shown) is comparable for the three arrays.

in the lower field intensity of the array. However, a decrease in array size produces enhanced field variation with distance, corresponding to larger gradient values. In the microarray, the net effect of smaller magnet volume and proximity of magnet poles is a gradient similar to that of the macroarray but a field intensity that is ~60 times smaller then that of the macroarray (see Table 2 and Appendix).

Adjustments in the distance between the magnets of the macroarray resulted in a gradient at the cell position equal to that produced by the microarray. Interpolation from Table 2 shows that, for a magnet separation of ~2.5 cm, a gradient of ~1.5 mT/mm for both arrays was obtained, with corresponding micro- and macroarray field strengths of ~0.1 mT and 6.8 mT, respectively. The number of AP failures in the fields of the two arrays did not differ significantly (Fig. 4).

Arrays with similar field intensities but significantly different field variations.

Similar field intensities for the macro- and microarrays were obtained by varying the distance between the magnets in the macroarray. For a magnet separation of ~75 mm, the macroarray experimental field strength was ~0.3 mT, and the corresponding field gradient value at cell location was ~0.02 mT/mm. This array configuration did not increase AP failures significantly (Fig. 5). In contrast, exposure to a weaker microarray field of ~0.15 mT, with a relatively large gradient of ~1.5 mT/mm, significantly increased the AP failures (Fig. 4, open squares).

No significant increase in AP failures was seen in neurons centered over single magnets with strengths of 0.5–500 mT. These results suggest that field magnitude in the examined range is insufficient to cause the biological effect and that field variation is the principal factor determining AP blockade.

Threshold Gradient Value

A decreasing magnetic field gradient was obtained experimentally by uniformly increasing the distances between magnets in the alternating four-macromagnet array. The experimental data on AP failures corresponding to different gradient values are shown in Figure 5. A precise threshold value for the gradient is difficult to establish for two main experimental reasons: 1) It is difficult to maintain a stable impalement of a single neuron long enough to perform measurements during exposure to multiple arrays with different gradient values and 2) because of variations in cell structure, different gradient values might be required to reduce firing in different neurons. With the present methods, we can determine only a gradient value at which the array field fails to block action potentials. As can be seen in Figure 5, a magnet separation of 75 mm, corresponding to a gradient of ~0.02 mT/mm, resulted in insignificant

TABLE 1. Measurements of the Horizontal Field Component B_{xy} Along Lateral (x,y) and Axial (z) Scanning Directions for the Microscopic Array and Measurement-Based Theoretical Estimates of Field Magnitude and Gradient of Field Magnitude*

Distance z (mm)	B_{xz} exp. (mT)	B_{xz} theo. (mT)	Distance x (mm)	B_{xx} exp. (at z = 1.5 mm; mT)	B_{xx} theo. (at z = 1.5 mm; mT)
1.5	0.08 ± 0.01	0.085	0	0.08 ± 0.01	0.085
2.5	0.04 ± 0.01	0.044	1	0.04 ± 0.01	0.039
3.5	0.02 ± 0.005	0.024	2	0.01 ± 0.005	-0.017
4.5	0.01 ± 0.005	0.013			
5.5	0.00 ± 0.005	0.007			

Distance y (mm)	B_{xy} exp. (at z = 1.5 mm; mT)	B_{xy} theo. (at z = 1.5 mm; mT)	Distance y (mm)	|B| theo. (mT)	Δ|B|/Δy theo. (mT)	Δ|B|/Δz theo. (mT)	Grad|B| theo. (mT/mm)
0.25	0.03 ± 0.005	0.032	0.5	0.07	0.77	0.92	1.07
0.75	0.09 ± 0.0	0.095	1	0.122	0.20	1.42	1.43
1.25	0.12 ± 0.01	0.121	1.5	0.128	0.08	1.31	1.31
1.75	0.09 ± 0.01	0.113	2	0.107	0.21	0.93	0.95
2.25	0.06 ± 0.01	0.089	2.5	0.08	0.22	0.56	0.60
2.75	0.04 ± 0.005	0.064	3	0.054	0.17	0.31	0.35
3.75	0.05 ± 0.005	0.028	3.5	0.036	0.12	0.16	0.20
4.75	0.20 ± 0.005	0.012	4	0.024	0.08	0.08	0.11

*exp. = experimental; theo. = theoretical.

TABLE 2. Characteristics of Magnetic Field at the Simulated Cell Location Produced by Macroarrays With Different Interpole Distances and the Microarray*

Distance between magnet centers (mm)	Cell location (x,y,z;) (mm)	Magnitude of measured field (B experimental; mT)	$\frac{\Delta\lvert B^{Exp}\rvert}{\Delta y}$ (mT/mm)	$\frac{\Delta\lvert B^{Exp}\rvert}{\Delta z}$ (mT/mm)	Grad($\lvert B^{Exp}\rvert$) (mT/mm) calculated	Magnitude of (mT/mm) field (B theoretical; mT)	$\frac{\Delta\lvert B\rvert^{TH}}{\Delta x}$ (mT/mm)	$\frac{\Delta\lvert B^{TH}\rvert}{\Delta y}$ (mT/mm)	$\frac{\Delta\lvert B^{TH}\rvert}{\Delta z}$	Grad ($\lvert B^{TH}\rvert$) (mT/mm)
1. Macroarray										
14	(0,4.5,6)	10	1.6	2.4	3.3	10	0.03	1.36	2.9	3.2
35	(0,12,6)	4.7	0.4	0.2	0.45	2.3	0.006	0.2	0.013	0.2
53	(0,18,6)	1.4	0.06	0.05	0.08	0.54	0.001	0.033	0.037	0.05
75	(0,25,6)	0.3	0.0025	0.018	0.018	0.14	0.000	0.006	0.014	0.014
2. Microarray										
0.4	z = 1.5 mm	$B_{x,max}$ at 1.5 mm above array ~0.12 ± 0.01 mT				0.15 mT max				~1.5 mT/ mm max

*For conciseness, we show only the experimental behavior of the field magnitude $|B^{Exp}|$ and gradient Grad($|B^{Exp}|$); because these are not directly measured quantities, we will indicate the procedure by which they are determined: One directly measures the three field components B_x, B_y, and B_z and their variations ($\Delta B_x^{Exp}/\Delta x$, $\Delta B_x^{Exp}/\Delta y$, $\Delta B_x^{Exp}/\Delta z$), ($\Delta B_y^{Exp}/\Delta x$, $\Delta B_y^{Exp}/\Delta y$, $\Delta B_y^{Exp}/\Delta z$), ($\Delta B_z^{Exp}/\Delta x$, $\Delta B_z^{Exp}/\Delta y$, $\Delta B_z^{Exp}/\Delta z$) in the neighborhood of the cell location. Measurements indicate that $0 \approx \Delta B_y^{Exp}/\Delta y \approx \Delta B_y^{Exp}/\Delta z \approx \Delta B_z^{Exp}/\Delta y \approx \Delta B_z^{Exp}/\Delta z \leq 0.05\ \Delta B_x^{Exp}/\Delta x$ at cell location; accordingly, we establish that $\Delta|B^{Exp}|/\Delta y = \Delta B_x^{Exp}/\Delta y$ and $\Delta|B^{Exp}|/\Delta z = \Delta B_x^{Exp}/\Delta z$. The quantities $\Delta B_z^{Exp}/\Delta x$ and $\Delta B_y^{Exp}/\Delta z$ are of the order of magnitude of $\Delta B_x^{Exp}/\Delta x$, and $\Delta B_x^{Exp}/\Delta x \approx 0$; the analytic behavior of the array points out that $0 \approx \Delta|B^{Exp}|/\Delta x \leq 0.05\ \Delta|B^{Exp}|/\Delta z$, thus indicating that $\Delta B_z^{Exp}/\Delta x$ and $\Delta B_y^{Exp}/\Delta x$ are opposing variations that mostly cancel out and generate an almost constant field magnitude along the x direction at cell location. For this reason, experimentally one cannot determine $\Delta|B^{Exp}|/\Delta x$ with a unidimensional probe, thus justifying the absence of $\Delta|B^{Exp}|/\Delta x$ from the table.

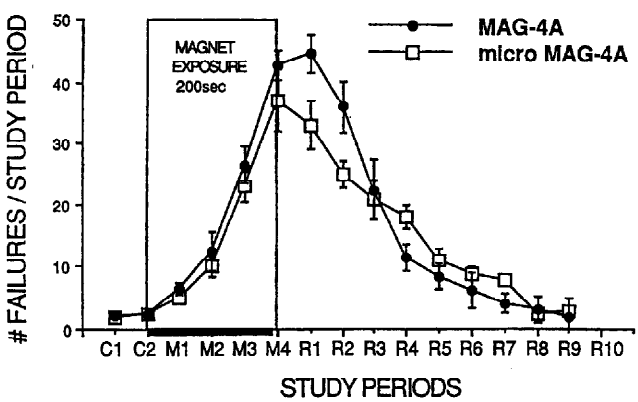

Fig. 4. Comparison of number of stimuli that failed to fire AP during exposure to fields produced by the micro- and macroarrays of four magnets of alternating polarity. Data collected for C-like neurons. At cell location, both arrays produced a field gradient of ~1.5 mT/mm and field intensities of ~6.3 mT and ~0.1 mT. Data from McLean et al. [1994], reexpressed graphically.

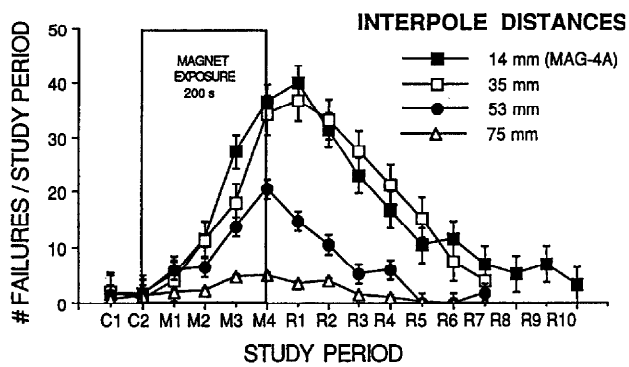

Fig. 5. Comparison between the inhibitory effects of the macroscopic array of four magnets of alternating polarity at different interpole distances d_i. Data were obtained by mounting magnets in plastic holders at center-center separations of 14, 35, 53, and 75 mm in square arrays. Cell located at (x,y,z) ~ (0, $1/3d_i$, 6 mm) measured from array center. Corresponding field amplitudes of 10, 4.7, 1.4, and 0.3 mT and field magnitude gradients of 3.3, 0.45, 0.08, and 0.018 mT/mm. Data from McLean et al. [1994], reexpressed graphically.

(<10%) reduction in AP firing. Thus, the threshold for AP blockade occurs at gradient values of ~0.02 mT/mm.

DISCUSSION

The experiments and analysis described herein were designed to discriminate which of two field characteristics, field intensity or gradient of the field magnitude, is the principal determinant of AP blockade in cultured neurons. The greatest number of failures to fire was observed in fields produced by arrays with the largest field gradients (Fig. 3, Table 2). Also, arrays of four magnets of alternating polarity with comparable gradients but an ~60-fold difference in field intensity ($B_{microarray}$ ~6 $B_{microarray}$) reduced AP firing to the same extent (Fig. 4). Theoretical estimates based on Lorentz force arguments require static constant field strengths in excess of 0.2 GT to affect action currents in nerves measurably [Liboff, 1980]. This prediction, made for time- and position-invariant fields, is consistent with our observations. Indeed, in our experimental range of 0.1–10 mT, we observed that fields with low gradient values have no significant effect on AP firing. On the other hand, the pronounced biological effect we observed in this intensity range occurs only if the time-independent magnetic field exhibits marked spatial variation. The present analysis suggests that field gradient, not intensity, is the principal determinant in action potential blockade.

As is indicated in Materials and Methods, due to the small size of the micromagnet, slight variations in cell positioning result in marked variability of the gradient to which the cell is exposed. If gradient dependent, the AP blockade in the microarray field should show location-dependent variation, as confirmed experimentally. Variability was much less with the macroarray, where larger magnet size permits more consistent cell positioning in a comparatively more slowly changing magnetic environment. Aside from variability in firing due to variations in the field gradient, our experiments indicate that neurons may discriminate between a strong unidimensional field variation and multidimensional field variations of lesser strength (see Appendix). For example, the MAG-2A array is characterized at cell position by a large transverse field variation [$(\Delta|B|/\Delta y) \cong 0.8$ mT/mm] and small longitudinal [$(\Delta|B|/\Delta x) \cong 0.005$ mT/mm] and vertical [$(\Delta|B|/\Delta z) \cong 0.1$ mT/mm] variations, with an overall gradient of ~0.8 mT/mm and no significant corresponding AP blockade. In contrast, the field of the MAG-4A array with interpole separation of 35 mm resulted in significantly more AP failures. This array had a slightly lower gradient value of ~0.5 mT/mm, but substantially different field variations [$(\Delta|B|/\Delta x) \cong 0.006$ mT/mm, $(\Delta|B|/\Delta y) \cong 0.4$ mT/mm, $(\Delta|B|/\Delta z) \cong 0.2$ mT/mm].

This example shows that the gradient of the field magnitude averages out the spatial variation of the individual field components and implicitly obscures component-dependent firing features. For this reason, the gradient of the field magnitude has to be regarded as a global indicator of field variation, not as a precise correlate of firing failure.

Although field intensity does not seem to be directly correlated with the extent of AP blockade, it is of general interest to determine whether a minimum intensity is required to at least allow the buildup of the field gradient necessary to block AP. Over 70% of stimuli failed to fire AP in experiments with arrays generating peak fields as low as 0.1 mT. For lower intensities, a theoretical intensity threshold can be obtained using the dependence of firing failures on the field gradient. Assuming that the effective gradient covers only part of the cell membrane, action potential-generating ion channels outside the field would still function properly, showing little if any failure in AP firing. For blockades similar to those observed experimentally, we then require a complete coverage of the neuronal membrane by the field gradient. Such coverage would require a field peak value of at least:

$$|\vec{B}_{min}| \approx |\mathrm{Grad}(B_{MAG})| \times \Phi_{CELL} \approx 0.5\,{}^{mT}/_{mm} \times 50\,\mu m \approx 0.025\,mT$$

where a standard cellular diameter of ~50 μm and an effective field gradient of ~0.5 mT/mm are used. This value is of the same order of magnitude as the terrestrial magnetic field.

Reports of effects of static magnetic fields in biological systems have come to widely varying conclusions. A uniform 1.2 T static magnetic field applied to voltage-clamped lobster axons [Schwarz, 1979] had no effect on conduction velocity, membrane potential, or transmembrane currents. On the contrary, consistent with our findings, rats changed direction to avoid regions of a T maze characterized by large changes in a static MRI field (up to 13 T/m for fields of ~1.7 T) [Weiss et al., 1992]. This suggests that living systems recognize and react to strong field changes. Accordingly, we believe that position-dependent field variations, in particular the gradient of field magnitude, must be assessed in future investigations of effects of static magnetic fields on cells or animals.

ACKNOWLEDGMENTS

The authors thank Mr. Ron Thomas for expert technical assistance with cell culture. This work was supported by a collaborative agreement between M.J.M., Vanderbilt University, and Holcomb Medical Research Institute.

REFERENCES

Landau L, Lifschitz E (1969): ["Electrodynamics of Continuous Media."] Moscow: Mir, p 168.

Liboff RL (1980): Neuromagnetic thresholds. J Theor Biol 83:427–436.

McLean MJ, Holcomb RR, Wamil AW, Pickett JD (1991): Effects of steady magnetic fields on action potentials of sensory neurons in vitro. Environ Med 8:36–45.

McLean MJ, Holcomb RR, Wamil AW, Pickett JD, Cavopol AV (1995): Blockade of sensory neuron action potentials by a static magnetic field in the 10 mT range. Bioelectromagnetics (16:20–32.).

Schwartz J-L (1979): Influence of a constant magnetic field on nervous tissues: II. Voltage-clamp studies. IEEE Trans Biomed Eng BME-26:238–243.

Weiss J, Herrick RC, Taber HK, Contant C, Plishker GA (1992): Bioeffects of high magnetic fields: A study using a simple animal model. Magn Resonance Imag 10:689–694.

APPENDIX

Gaussmeter Characteristics

The FW Bell gaussmeter 4048 has an active measurement window of diameter d = 0.5 mm. It is calibrated in a uniform field with the active measurement area $\approx \pi \times 0.06\ mm^2$ taken to be unity. For nonhomogeneous fields that change rapidly over the size of the active window, corrections to the instrument reading have to be applied. An example will clarify the necessity for such corrections: An idealized field of amplitude 1 mT that is constant over half of the active window and zero elsewhere will give an instrument reading of only 0. 5 mT. Alternatively, for a fluctuating field, the instrument reading corresponds to $B_{G.meter,z} = \iint rdrd\phi B_z(r,\phi,z)$. For the z component of a field produced by one cylindrical magnet scanned at constant height (z = 1.5 mm), which displays angular symmetry, the above formula reduces to

$$B_{G.Meter,Z}(z=1.5) = 2\pi \int_0^{2.5} rdrdB_z(r,1.5)$$

$$\equiv \sum_{i=0}^{n} B_z(r_i,1.5)\delta A_i$$

is the annular area that corresponds to the field $B_z(r_i,1.5)$ for the chosen partition i]. For a six-point partition sum at the cell height for one micromagnet, the discrepancy between instrument reading and field value at a site was small (only 4% difference); at magnet surface, the same sum gives a larger discrepancy (30% difference).

The instrument reading in areas of slow field change is accurate to at least 95% at the experimental cell height; in areas of fast field change the reading is less reliable and depends on the rate of change of the field. For example, the B_{xy} field component scanned in the y direction (relatively low field change; Fig. 6a), registers a peak value of ~0.12 mT. The same field component scanned in the x direction registers a peak value of only $B_{xx,max}$ ~0.09 mT. The instrument average over the large field variation in the x direction (0.74 mT drop over 0.2 mm; Fig. 6b) causes the lower reading.

The degree of alignment among probe and sample determines the percentage measurement between the targeted field component and the other field components. Accordingly, reliable field measurements are obtained in areas where the target field component is much larger then the other two components. In areas where the targeted field is small in comparison to the other components, readings are unreliable. For example, in measurements of B_{xx} (Table 1), a slight shift in the orientation of the probe and the large z field component result in a theoretical value (-0.017 mT at 2 mm) largely discrepant from the measured value (0.01 mT at 2 mm).

Characteristics of the Microarray Field

The microarray diameter of ~0.8 mm was similar to the gaussmeter measurement window diameter of ~0.5 mm. Thus, the active measurement window of the probe effectively averages and limits spatial resolution of the field strength. A reliable reading is produced by a field component that does not change sign over the active measurement area and is sufficiently uniform to allow for corrections to the averaging of the instrument. The axial (B_z) field measured at the array surface changed from a peak value of ~4 mT to -4 mT over a distance of ~0.4 mm. The corresponding averaged reading of ~0.1 mT is a substantial distortion in local field value. Consequently, we measured and modeled the $B_{x(y)}$ component of the microarray field, which displays the least sign change over the active measurement area, when scanned at constant height. Therefore, the computer simulation was calibrated to best fit the measurements of B_x taken along the x, y, and z directions. The analytical model was used to characterize the field further. Measured and simulated data for B_x are displayed in Table 1 and the corresponding field maps in Figure 6. Some of the important analytic features of the array and the motivation for the choice of the particular component to be measured are given below:

1. Compared to the z field component, the $B_{x(y)}$ component keeps the same sign over a larger scanning area, allowing more accurate readings.

2. The locations at which B_x is maximal correspond to null contributions from B_y and B_z. Thus $B_x(0,y,1.5) = B_{x,MAX} = |\vec{B}(0,y,1.5)|$; i.e., the magnitude of the field coincides with the value of the component along the whole y axis at x = 0.

3. The model parameters set by the fit between measured and computed values of the x field component (Fig. 6a,b) are used to predict a field magnitude range

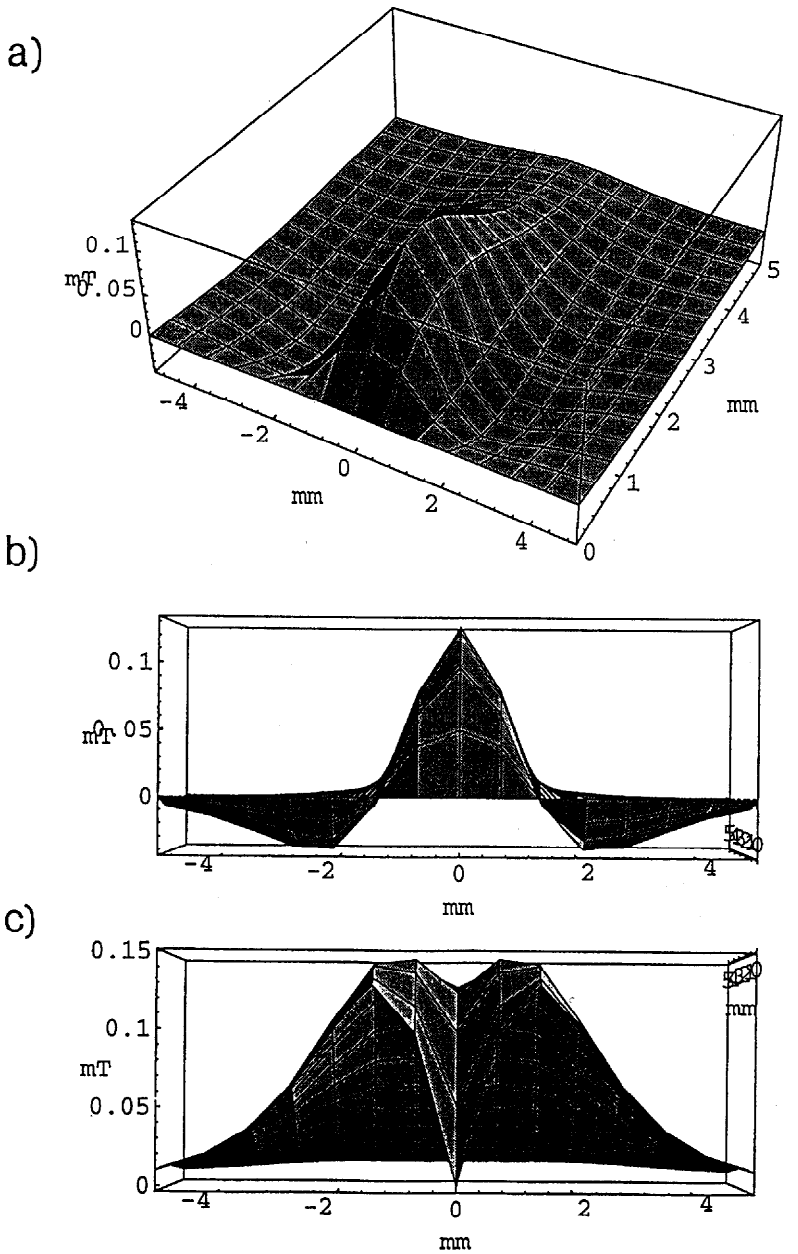

Fig. 6. Simulated surface plot of the microarray field. **a,b:** Side views of the B_x component for z = 1.5 mm; the measured and corresponding analytic plot values are shown in Table 1; the plot covers only half of the domain, with the field symmetrical and of opposite sign in the other half. **c:** Sectional view of the analytical field magnitude corresponding to the measured values of B_x; this field magnitude is used to calculate the unidimensional variations and gradient of the field in Table 1.

between 0 (background) and 0.13 mT and a gradient range between 0.3 and 1.4 mT/mm at z = 1.5, x = 0, and y = 0–5 mm.

4. The maximum field magnitude and gradient occur along the line that connects the geometrical center of the array with any magnet center. At these particular locations, the maximum field amplitude is ~0.15 mT, the vertical field variation ~1.7 mT/mm, and a radial field variation ~0.04 mT/mm, resulting in a gradient of ~1.7 mT/mm. In the area of the inner cone (Fig. 6c) along this same direction, for a field amplitude of ~0.12 mT, the vertical field variation of ~1.4 mT/mm

and a radial field variation of ~0.8 mT/mm result in a gradient of 1.6 mT/mm.

5. Alternatively, measurements of the field produced by a single micromagnet were used to calculate microarray characteristics. The values obtained for the array, of ~1.7 mT maximum field amplitude and ~1.2 mT/mm maximum gradient at cell height are in agreement with the corresponding values obtained from measurements of B_x.

6. Table 1 shows that regions characterized by the same gradient correspond to different variations with position of the individual field components (see number 4 above, for example). This particular feature of the field may explain, at least in part, the variability in AP block observed for the microarray.

Error Analysis

Each of the field components was measured by appropriate orientation of the gaussmeter probe in the field. For each orientation (field component), the field was scanned along the three axes shown in Figure 1. The three scanning directions intersected at a site corresponding to the cell position in the field. Relative to the center of the quadrupolar array, the positioning range of the cell during magnetic exposure and AP recording was $(x,y,z) = (0 \pm 1\ mm,\ 4.5 \pm 1\ mm,\ 6 \pm 1\ mm)$. The field measurements and associated errors are shown in Table 3. In the notation B_{ij}, the first subscript identifies the field component (x, y, or z) and the second one labels the direction of scanning (i.e., along the x, y, or z axis).

The sources of measurement error are mentioned in Materials and Methods. Error stemming from misalignment of axes might have introduced deviations up to 1° of arc. In our apparatus, misalignment could produce deviations of as much as 0.2 mm for every centimeter scanned. In areas with large field variation, a maximal error of 15 mT/mm of deviation, not surpassing 30% of the field value at a particular location, might occur. Relative to the angular misalignment error, the most accurate measurements are the ones taken in the vicinity of the intersection of the manipulator axes, a location that corresponds to the site of the neuron under study. Accuracy decreases at larger distances from the origin, where field intensity diminishes gradually to negligible values. A 10% error for reading the vernier rulers was included in the estimate of systematic error, and values were rounded up to the nearest significant integer or decimal number.

The error is calculated according to $\varepsilon_{ij} = l_j \times 0.018 \times \Delta B_j/\Delta x_j + 10\% \times \Delta B_i/\Delta x_j \times \Delta x_j$, where l_j is the length along the jth scanning direction and measured from the cell location, $\Delta B_i/\Delta x_j$ is the field's ith component variation along the j direction, 0.018 is the radian conversion of the 1% angular deviation, and 10% is the caliper reading error mentioned in the text. Throughout the measurements, Δx_j was 1 mm. The errors are rounded up to the closest relevant integer.